Nanoscale

PAPER

View Article Online
View Journal | View Issue

Cite this: *Nanoscale*, 2019, **11**, 19877

Probing surface mediated configurations of nonplanar regioisomeric adsorbates using ultrahigh vacuum tip-enhanced Raman spectroscopy†

Sayantan Mahapatra, [a] Jeremy F. Schultz, [a] Yingying Ning,[b] Jun-Long Zhang [b] and Nan Jiang *[a]

The ability to directly probe the adsorption configurations of organic regioisomeric molecules, specifically nonplanar isomers, on well-defined substrates holds promise to revolutionize fields dependent on nanoscale processes, such as catalysis, surface science, nanotechnology and modern day electronic applications. Herein, the adsorption configurations and surface sensitive interactions of two nonplanar regioisomer, *trans*- and *cis*-tetrakispentafluorophenylporphodilactone (*trans*- and *cis*-H_2F_{20}TPPDL), molecules on (100) surfaces of Ag, Cu and Au were studied and investigated using high resolution scanning tunneling microscopy (STM), combined with ultrahigh vacuum tip-enhanced Raman spectroscopy (UHV-TERS). Depending on molecule–substrate interactions, similar "phenyl-up" configurations were observed for these molecules on Ag(100) and Au(100), while a "phenyl-flat" configuration was discovered on a Cu(100) surface. With the help of surface selection rules of TERS, we explain the spectral discrepancies recorded on the Ag and Cu substrate. Furthermore, the intermolecular interactions were addressed using STM analysis on these surfaces after the configurations were determined by TERS. This study sheds light on the distinct configurations of regioisomeric porphodilactone systems (at interfaces) for near-infrared (NIR) photosensitizers and molecular electronics in the near future.

Received 8th August 2019,
Accepted 19th September 2019

DOI: 10.1039/c9nr06830a

rsc.li/nanoscale

Introduction

Investigation of the adsorption configurations of nonplanar organic molecules on different well-defined surfaces holds promising applications in surface sciences, catalysis, and various fields in nanotechnology. The configuration of surface adsorbed molecules plays an important role in tailoring the properties of self-assembled monolayers (SAMs) and governs the performance of modern-day electronic devices.[1] Significant charge transfer with the substrate may result in distinct surface packing and lead to completely different configurations for the surface-bound molecules.[2] These molecule–substrate interactions can limit the diffusivity of the adsorbed molecules, modify the electronic structure, and also alter the configuration. The substrate thus turns into an intriguing parameter to manipulate the self-assembly and configurations of adsorbed molecules. Therefore, it is critical to elucidate the effects of different supporting substrates on the adsorbed configurations and self-assemblies of the molecular system.

Tetrakispentafluorophenylporphodilactone (H_2F_{20}TPPDL), represents a porphyrin like structure where the lactone moieties take the place of peripheral bonds of two opposite pyrrole rings[3] and has attracted considerable attention due to its promising applications in near-infrared (NIR) photosensitization,[4] triplet–triplet annihilation,[5] lanthanide sensitization,[6] and so forth. This type of molecule *i.e.* four flexible phenyl ($-C_6F_5$) ligand rings attached to the PDL core, can adopt nonplanar complex adsorption configurations on different substrates mainly as a result of molecule–substrate interactions, which also influence their electronic, chemical and photophysical properties.[2,7] Therefore, it is of immense interest to understand the complete picture of these nonplanar molecular systems at the level of the single molecule when they are adsorbed on different metal substrates. Scanning probe techniques such as scanning tunneling microscopy (STM) and non-contact atomic force microscopy (nc-AFM) have spatial

[a]*Department of Chemistry, University of Illinois at Chicago, Chicago, Illinois 60607, USA. E-mail: njiang@uic.edu*
[b]*Beijing National Laboratory for Molecular Sciences, College of Chemistry and Molecular Engineering, Peking University, Beijing 100871, P. R. China*
†Electronic supplementary information (ESI) available. See DOI: 10.1039/c9nr06830a

resolution down to single chemical bonds.[8,9] These techniques work extremely well with planar molecules. However, to completely characterize nonplanar molecules, advanced surface techniques must be applied. Since its discovery, tip-enhanced Raman spectroscopy[10] (TERS) has been extensively used as a powerful tool for optical microscopy with high sensitivity and spatial resolution.[10–17] Because of its highly confined plasmonic field and high enhancement of Raman signal directly under the tip apex, different molecules,[18,19] even adjacent regioisomers,[20] can be distinguished with angstrom scale precision. Therefore, STM combined with TERS can be an ideal tool to analyze the system at the nanoscale. At different interfaces, these *trans*/*cis*-regioisomers in which a small structural change is fabricated inside the molecular central core (ESI: Fig. S1a†) are extremely crucial for analyzing regioselective heterogeneous catalysis reactions, molecular electronics, *etc*. However, the complementary techniques of STM and TERS have yet to be applied to investigate the self-assembly and different complicated configurations of these nonplanar isomeric pairs on three well-defined substrates simultaneously.

In this article, we report topological and chemical insights into *trans*- and *cis*-H_2F_{20}TPPDL on Ag(100), Cu(100) and Au (100), three different single crystals using high resolution STM and, ultrahigh vacuum (UHV) TERS. Selection of fully fluorinated molecules (twenty C–F groups in the phenyl rings) has obvious advantages over their non-fluorinated counterparts as the C–F group exhibits strong and easily detectable characteristic Raman features in the 500–800 cm^{-1} region.[21] Furthermore, TERS selection rules can be applied to resolve different nonplanar configurations of a molecule due to not only the tensor properties of Raman scattering, but also the directional (vector) nature of the highly confined plasmonic field parallel to the tip axis.[22–24] Following that, molecule–molecule interactive information such as the involvement of functional groups into the self-assembly formation and distances between molecules inside the assembly is analyzed using STM study. Therefore, this study can be an ideal platform not only to establish the configuration–interaction relationships of nonplanar molecules with different supporting metal substrates but also to understand the manipulation of self-organized assemblies by a subtle change in the central part of the molecule (as in this case of *trans*/*cis* isomers, alternating the carbonyl groups, Fig. S1a†), which may become very useful in engineering self-assembly and catalytic reactions at the nanoscale.

Results and discussion

In general, this type of porphyrin molecule exhibits multiple electronic transitions[25] in the near ultraviolet (UV) and visible region as shown in the absorption spectra in Fig. 1a and Fig. S1b,† which were recorded from *trans*-molecules dissolved in dichloromethane (DCM). It reveals a strong electronic excited state (near-UV), known as a Soret band (Fig. S1b†), and four Q bands such as $Q_x(0,1)$, $Q_x(0,0)$, $Q_y(0,1)$ and $Q_y(0,0)$ in

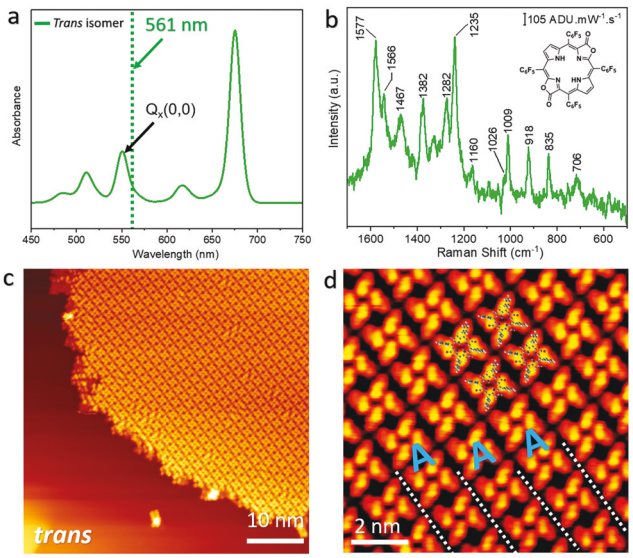

Fig. 1 (a) Visible absorption spectra of *trans*-H_2F_{20}TPPDL in dichloromethane (DCM) at 298 K. (b) TERS fingerprint for *trans*-H_2F_{20}TPPDL on Ag(100) using a 561 nm laser. Tip-retracted signal is subtracted from the tip-engaged signal. Tip-engaged and tip-retracted spectra are highlighted in the ESI (Fig. S2†). (Inset) Chemical structure of *trans*-isomers. (c) Large-scale STM image of *trans*-H_2F_{20}TPPDL deposited on Ag(100). (d) Zoomed-in view of *trans*-isomers which indicates "AAA"-type packing. Models of *trans*-isomers are superimposed.

the visible region (Fig. 1a). Comparing the Q bands observed in solution and in a thin layer, no significant shift was detected (Fig. S9†),[16] for example, the $Q_x(0,0)$ band shifts from 552 nm (in solution) to 556 nm (on surface) for *trans*-isomers (Fig. S9†), therefore a 561 nm laser source was chosen (green dotted line in Fig. 1a) to investigate the $Q_x(0,0)$ electronic excited state for *trans*-isomers. This can lead to greatly enhanced intensity of Raman scattering due to frequency coincidence (resonance). We maintain the same laser excitement (561 nm) for *trans*-H_2F_{20}TPPDL molecules on all three different substrates *i.e.* Ag(100), Cu(100) and Au(100) as this can offer us an opportunity to interpret the modification of the TERS signal as an effect of changing the underlying substrate.

The *trans*-H_2F_{20}TPPDL molecules were deposited on the Ag(100) substrate at room temperature with sub-monolayer coverage. The identification of multiple vibrational peaks by using TERS allows us to have precise chemical information of the surface adsorbed molecules at the nanoscale. Fig. 1b represents the TERS fingerprint of *trans*-H_2F_{20}TPPDL molecules acquired with 561 nm laser irradiation, while the tip scans over molecular islands. We have also presented tip-retracted flat spectra in the ESI (Fig. S2†) to ensure that the Ag tip was not contaminated and that the signals originate from molecules adsorbed on the Ag(100) substrate. Generally, TERS follows the surface-enhanced Raman spectroscopy (SERS) selection rules,[26] which suggest that only those modes parallel to the tip axis are highly enhanced.[23,24] In our case, the hydrogen atoms on the phenyl rings are substituted by fluorine

atoms; these C–F groups, which exhibit peaks in the Raman spectrum in the 500–800 cm^{-1} range, can be crucial in determining the surface adsorbed configurations. The 500–800 cm^{-1} spectroscopic region can be tracked easily to resolve C–F vibrational modes (considering the selection rules) as it directly relates to the relative orientation of the phenyl ($-C_6F_5$) rings. Some peak features in this region suggest that the phenyl ($-C_6F_5$) rings stand up on the surface, leading to a "phenyl-up" configuration. Conversely, a silent zone (no peak features) indicates that the phenyl ($-C_6F_5$) rings lie flat, leading to a "phenyl-flat" configuration. On Ag(100), we noticed peak features in that region (Fig. 1b), suggesting that the phenyl ($-C_6F_5$) rings are uplifted from the Ag substrate. Note, since the excitation laser source is polarized parallel to the tip axis, the plasmon enhanced electric fields that are generated under the tip apex are perpendicular to the flat Ag(100) substrate. Therefore, in the case of Raman scattering, the intensity of the Raman signals is likely to be much higher for the out of plane vibrational modes as they match the orientation of the enhanced electric field.[24] This is the reason why we observed signals that correspond to the phenyl ($-C_6F_5$) rings in this "phenyl-up" configuration in the 500–800 cm^{-1} region. In accordance with previous studies done on similar types of molecules *i.e.* metallated or non-metallated tetraphenylporphyrin (M-TPP/H_2-TPP) on Ag surfaces, we define this "phenyl-up" configuration as a "pinwheel" configuration for our molecules,[20,27] which is slightly deformed in shape compared to the gas phase structure.[3]

The detailed packing behaviour of *trans*-H_2F_{20}TPPDL on Ag (100) was studied with a constant current STM experiment. In our experiment, we rarely observed isolated molecules separate from self-assemblies, indicating strong intermolecular interactions. The surface diffusion of adsorbed molecules is firmly constrained by neighbouring molecules and attractive molecule–molecule interactions leading to the formation of highly ordered structures, as shown in Fig. 1c. Fig. 1d shows a zoomed-in view of these extended 2D networks of *trans*-isomers in which they show a "regular" arrangement, leading to "AAA"-type of packing. In Fig. 1d, individual molecules can be clearly identified, and a few scaled *trans*-molecules are superimposed. As our TERS study already confirms the "phenyl-up" configuration for those molecules on Ag(100), we should expect the phenyls ($-C_6F_5$) to appear elevated in apparent height compared to the core. However, as we try to match the gas phase model of these molecules with the STM image (in Fig. 1d), the phenyl ($-C_6F_5$) rings appear relatively dimmer than the other part of the molecule. This can be explained by the fact that the topographic features obtained from STM are mainly determined by the local density of states (LDOS) of the molecule not the real height. This indicates that TERS provides convincing information about the adsorption configuration of nonplanar molecules, whereas STM alone is not capable of it.

Following that, we used the same experimental method to investigate the molecular adsorption behaviours of *trans*-H_2F_{20}TPPDL molecules on the Cu surface. In order to avoid different surface facets which can lead to different surface superstructures, we chose Cu(100) as the substrate. Deposition parameters were kept identical to obtain similar coverage. Fig. 2a depicts the vibrational fingerprint (TERS spectrum) of these molecules, acquired with a 561 nm laser source. The fingerprint of these molecules on Cu(100) appears to be completely distinct compared to what was observed on Ag(100), with a flat 500–800 cm^{-1} spectroscopic region. This change in the spectrum suggests a different molecular configuration on the Cu substrate with the phenyl ($-C_6F_5$) rings staying parallel to the surface, indicating a "phenyl-flat" configuration for *trans*-isomers.

After the configurations of individual nonplanar *trans* adsorbates were determined, STM experiments of these molecules were utilized on Cu(100) to understand the molecule–molecule interactions in detail. Compared to the Ag(100) substrate, we found self-organized assemblies of these molecules on Cu(100) with different packing arrangements. Generally, this type of tetraphenylporphyrin molecule can be found as randomly oriented and isolated from neighbouring molecules on the Cu substrate at sub-monolayer coverage due to strong molecule–substrate interactions and negligible intermolecular interactions.[2,28] The migration barrier of porphyrin molecules for surface diffusion on Cu is relatively high compared to that on an Ag substrate[29] and the dipolar moments caused by charge transfers between molecules and the substrate can be responsible for that.[30] However, the observation of 2D assemblies (Fig. 2b) suggests that attractive molecule–molecule interactions overcome this migration barrier. The large scale STM image (Fig. 2b) indicates that they also took a similar "AAA"-type arrangement on Cu(100). In our experiment, we were able to resolve the fine structure and a single molecule is identified by a white dotted rectangle in Fig. 2c. The configurational information appears to be topologically distinct on Cu(100) in contrast to what was seen on Ag(100). We observe bright protrusions in the central part of the molecule (four dotted white circles in Fig. 2c), whereas relatively dimmer features appear on the outside of the PDL core (four dotted white arrows in Fig. 2c), indicating a completely different configuration on Cu (100) compared to the configuration of these molecules on the Ag(100) substrate. This explains the observed alteration in the whole TERS spectrum. Moreover, this distinct "phenyl-flat" configuration is further confirmed by fingerprint analysis in which the 500–800 cm^{-1} range is silent for the *trans*-isomers. We define this certain geometry as an "inverted" configuration for our molecules.[7] The different configurations of these molecules adopted on different substrates reveal the clear impact of the underlying surface on the geometry of the molecules. With flat phenyl ($-C_6F_5$) rings, these self-organized assemblies were stabilized due to an extended halogen bonding network with C–F···F type of attractive interactions. Recently, Kawai *et al.* defined this type of extended halogen bonding for a flat fully fluorinated molecule on a Ag(111) substrate,[31] where they discussed a few important computational conclusions. These halogen bonding interactions were found to be the strongest at an optimal F···F distance of ~3.1 Å and when the C–F···F unit appears in a straight line.[31] Based on the STM topograph and

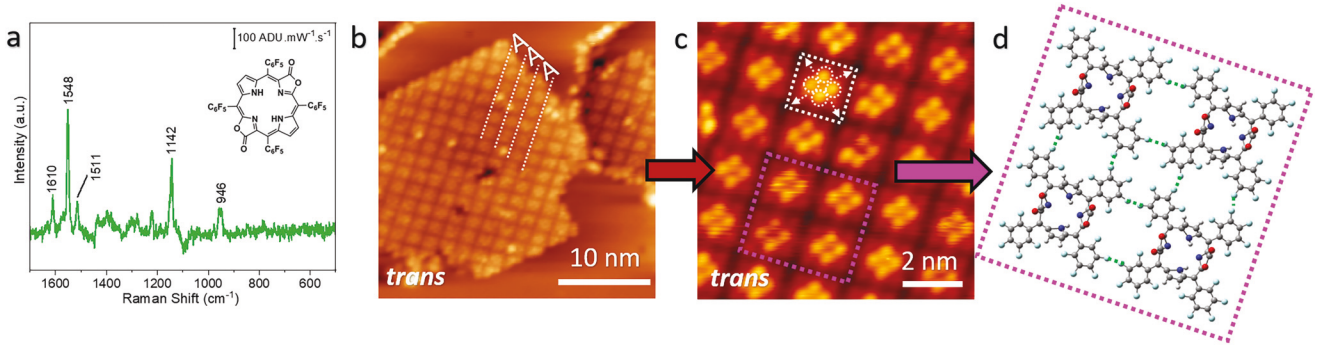

Fig. 2 TERS and STM study of *trans*-H_2F_{20}TPPDL on Cu(100). (a) TERS fingerprint for *trans*-isomers on Cu(100) with a 561 nm laser source. Tip-retracted signal is subtracted from the tip-engaged signal. Tip-engaged, tip-retracted spectra are highlighted in the ESI (Fig. S3†). (Inset) Chemical structure of *trans*-isomers. (b) Large-scale STM image of *trans*-H_2F_{20}TPPDL on Cu(100) indicating a "AAA"-type arrangement. (c) Zoomed-in view of *trans*-isomers in which a single molecule is identified by a dotted white rectangle. The dotted white circles signify the central part (four pyrrole rings) and dotted white arrows suggest outside of the core (four phenyl rings). (d) A tentative model of *trans*-isomers (from the area marked by pink dotted rectangle in Fig. 2c) where a few C–F···F interactions are highlighted.

TERS results, we propose a tentative model for *trans*-isomers in Fig. 2d in which a few C–F···F interactions are highlighted. The proposed model indicates multiple linear C–F···F linkages along with possible angled interactions with an average distance of ~3.15 ± 0.15 Å between the fluorine atoms (marked by the green dotted line in Fig. 2d and Fig. S4†), in line with previously calculated results.[31]

After that, we investigated the other regioisomeric counterpart, *cis*-H_2F_{20}TPPDL on Ag(100) and Cu(100) surfaces respectively. In the case of *cis*-isomers, we chose 633 nm laser excitation to probe the $Q_y(0,0)$ electronic band as shown with the red dotted line in Fig. 3a, and kept the same laser excitation (633 nm) on all the different surfaces due to the reason mentioned before. We deposited *cis*-H_2F_{20}TPPDL on these two clean substrates to obtain sub-monolayer coverage. Fig. 3b describes the TERS signatures of these molecules obtained with a 633 nm laser in which the top panel (pink) depicts the spectrum on Ag(100), whereas the bottom panel (red) is on Cu(100). Like the behaviour of *trans*-isomers on these two substrates, peak features were identified for *cis*-isomers on Ag(100) in the 500–800 cm^{-1} region, whereas no signature was observed on the Cu(100) surface in that concerned region (Fig. 3b). We conclude that the *cis*-isomers also took a "phenyl-up" configuration on Ag(100), whereas they adopted a "phenyl-flat" configuration on Cu(100). Note, the spectral variation (such as peaks of Raman shift) observed on Ag(100) and Cu(100) for these two isomers are not due to probing different electronic states, as we keep the same laser excitation for the *trans* isomer on the Ag, Cu surface and the same goes for *cis*. However, in comparison with the *trans*-isomers on Ag(100), the self-arrangement for the *cis*-isomers becomes very different on Ag(100) as seen in Fig. 3c. Switching the lactone moieties in the chemical structure induces a "zig-zag" pattern in which they establish "ABA"-type packing, and the B molecular row is rotated ~50° compared to molecular row A (Fig. 3c and d). The closer packing pattern reveals significant contributions of the lactone moieties that interact with the phenyl ($-C_6F_5$) rings of

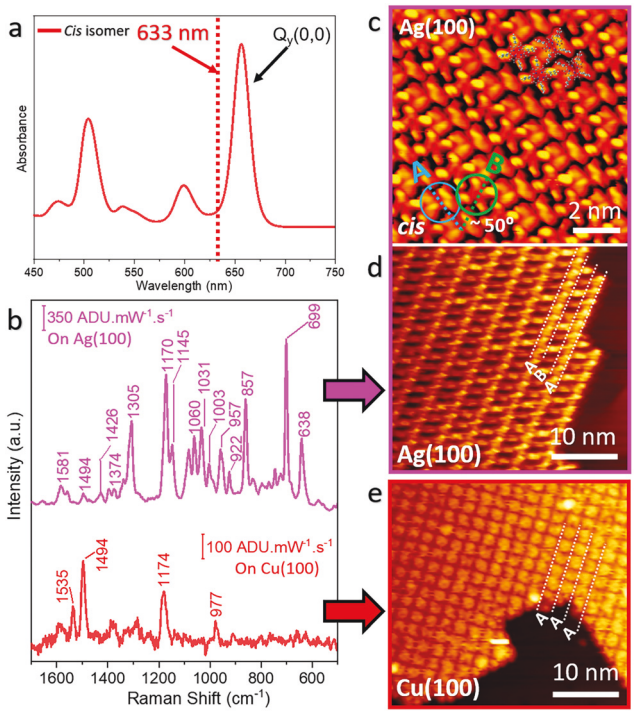

Fig. 3 TERS and STM study of *cis*-H_2F_{20}TPPDL on Ag(100) and Cu(100). (a) Absorption spectra of *cis*-isomers in dichloromethane (DCM) at 298 K. (b) TERS fingerprint for *cis*-H_2F_{20}TPPDL on Ag(100) [top panel, pink] and Cu(100) [bottom panel, red] using a 633 nm laser. Tip-retracted signal is subtracted from the tip-engaged signal. Tip-engaged and tip-retracted spectra are highlighted in the ESI (Fig. S5†). (c) Zoomed-in STM image of *cis*-H_2F_{20}TPPDL deposited on Ag(100) in which molecular row B rotates ~50° compared to A rows. Models of *cis*-isomers are superimposed on the image. (d) Zoomed-out view of *cis*-isomers on Ag(100) which indicates "ABA"-type packing. (e) Large scale STM image of *cis*-isomers on Cu(100) which shows "AAA"-type packing.

adjacent molecules in the self-assembly, as shown in Fig. 3c with a few model *cis*-molecules. This also incorporates irregularity into the packing. In contrast to the packing behaviour of

cis-isomers on Ag(100), they took the regular "AAA"-type arrangement on Cu(100) as shown in Fig. 3d and e using large-scale STM images. In other words, the *trans*- and *cis*-isomers took "AAA"-type and "ABA"-type packing respectively on Ag(100), whereas both adopted a similar "AAA"-type arrangement on Cu(100). A similar behaviour of *trans*- and *cis*-isomers on Cu(100) suggests that the lactone moieties (in the pyrrole rings) make negligible contributions in the self-assembly formation, whereas the phenyl ($-C_6F_5$) rings are directly involved. We conclude that since the phenyls ($-C_6F_5$) are flat on the Cu(100) surface, only the phenyl ($-C_6F_5$) rings take part in the self-assembly process through attractive halogen–halogen (fluorine) interactions which results in similar "AAA"-type packing for both of the molecules. Particularly, in the case of *cis*-isomers, the tentative model (Fig. S6†) shows that major attractive interactions exist between the lactone moieties and the adjacent phenyl ($-C_6F_5$) rings on Ag(100). However, on Cu(100), the prominent interactions occur between adjacent phenyl ($-C_6F_5$) rings due to the "inverted" configuration (Fig. S6†).

We also deposited these molecules separately on Au(100) at room temperature. The topological information is summarized in Fig. 4a and b for *trans*- and *cis*-isomers respectively. However, the (100) facet of the Au surface is not flat compared to Ag(100) and Cu(100) as the "Au(100)-hex" reconstruction takes place and can be clearly seen in Fig. 4a and b on the bare Au substrate.[32] The STM images clearly show obvious differences inside the self-assembly for *trans*- and *cis*-isomers, whereas the packing and configuration of these molecules becomes very ambiguous. These molecules inside the molecular islands reveal spatially resolved internal structure as indicated in the inset of Fig. 4a and b which suggests significant electronic decoupling of these molecules from the supporting substrate. Decoupling of the molecules from the substrate is very desirable to investigate the intrinsic electronic properties of molecules and generally can be achieved using passivated surfaces,[33] ultra-thin insulating films on the metal surfaces,[34] molecular buffer layers,[35] or specific weakly adsorbed (physisorbed) organic molecular systems on metallic surfaces.[36] Therefore, we conclude, as a result of weak molecule–substrate interactions for these molecules on Au(100), STM was able to resolve the internal features of the molecules. However, the self-assembly and the adsorption configuration of the molecules remain uncertain.

In order to determine the configuration of adsorbed molecules, as well as the effect of surface sensitive interactions on the Au(100) substrate, we performed TERS experiments under 561 nm (*trans*) and 633 nm (*cis*) laser irradiation. Fig. 4c and d depict the chemical identification (TERS fingerprints) of *trans*- and *cis*-isomers respectively on Au(100). Peak features in the previously discussed 500–800 cm^{-1} region were observed which suggests that these molecules took a "phenyl-up" configuration on Au(100). Furthermore, we compare the whole spectra of these two isomers that were acquired on these two different substrates [Ag(100) and Au(100)] *i.e.* Fig. 1b and 4c (for *trans*-isomers) and Fig. 3b (top panel) and 4d (for *cis*-isomers), and observed good agreement in the fingerprint regions, in terms of peak positions and intensities (ESI, Fig. S8†). This indicates that they adopt a similar "pinwheel" configuration on Au(100) to that on Ag(100). Although the surface adsorbed configurations of these nonplanar regioisomeric molecules remained unclear with STM, these configurations can be studied precisely by their fingerprint analysis using STM-TERS.

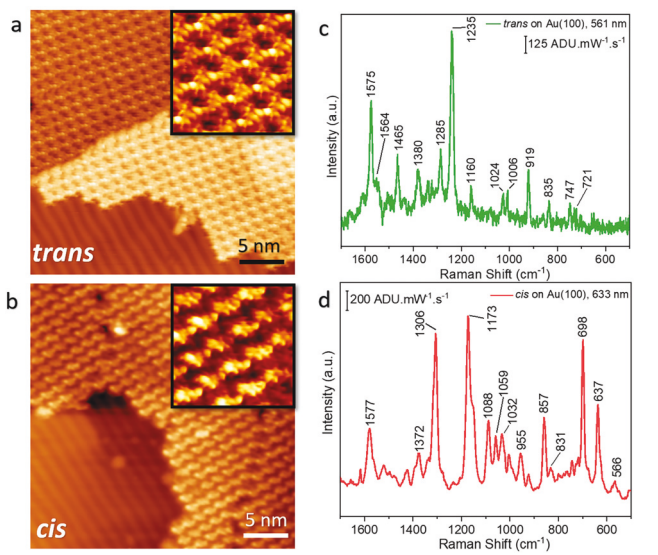

Fig. 4 TERS and STM study of *trans*- and *cis*-H_2F_{20}TPPDL on Au(100). (a) STM topograph of *trans*-isomers. (Inset) Zoomed-in image (12 nm × 12 nm). (b) STM image of *cis*-isomers. (Inset) Zoomed-in image (12 nm × 12 nm). (c) TERS fingerprint for *trans*-H_2F_{20}TPPDL using a 561 nm laser. (d) TERS fingerprint for the *cis*-H_2F_{20}TPPDL with a 633 nm laser source. Tip-retracted signal is subtracted from the tip-engaged signal. Tip-engaged and tip-retracted spectra are highlighted in the ESI (Fig. S7†).

Conclusions

Taken together, using TERS combined with STM analysis, we can chemically identify the adsorption configurations of nonplanar regioisomeric molecular systems on three different surfaces accurately and precisely. Our analysis confirms that these regioisomeric pairs (*trans*- and *cis*-PDL) took similar "phenyl-up" configurations on Ag(100) and Au(100), whereas a "phenyl-flat" configuration was identified on Cu(100). The ability to investigate the adsorption configuration of nonplanar regioisomers with STM-TERS, as demonstrated here, holds broad and diverse applications in various fields of surface chemistry ranging from molecular electronic devices to selective heterogeneous catalysis reactions, single molecule study, and beyond. Furthermore, this study provides practical insights into the different configurations of these new PDL systems (at different interfaces), which is a necessity for the development of new materials for electronic bio-sensing, and so forth.

Experimental methods

Sample preparation and analysis took place using an STM system (Unisoku) at a base pressure of $<1 \times 10^{-10}$ torr. The samples were cooled to liquid nitrogen temperature (~78 K) for STM and TERS experiments. An electrochemically etched Ag tip (plasmonically active) was cleaned in UHV by Ar^+ sputtering (1.5 kV, $\sim 2.5 \times 10^{-5}$ torr). All the single crystals *i.e.* Ag(100), Au(100) and Cu(100) were prepared with repeated cycles of Ar^+ sputtering (1 kV, $\sim 2.5 \times 10^{-5}$ torr), followed by annealing at 800 K, 865 K and 840 K respectively. *trans*- and *cis*-H_2F_{20}TPPDL molecules, prepared according to the literature,[3] were sublimed onto clean single crystals with a molecular evaporator held at ~500 K to obtain sub-monolayer coverage at room temperature. TERS signals were detected with excitation from 561 nm (for *trans*) and 633 nm (for *cis*) continuous wave (CW) laser irradiation (LASOS). An Iso-Plane SCT-320 spectrometer (Princeton Instrument), equipped with a Princeton Instrument PIXIS 100 charged coupled device (CCD), was used for TERS experiments. A detailed description of our home built experimental TERS set up can be found in a previous publication.[37]

Conflicts of interest

The authors declare no competing financial interest.

Acknowledgements

N. J. acknowledges financial support from the National Science Foundation (CHE-1807465). J. L. Z. acknowledges financial support from the National Scientific Foundation of China (No. 21778002, 21621061 and 21861162008).

References

1 J. N. Hohman, P. Zhang, E. I. Morin, P. Han, M. Kim, A. R. Kurland, P. D. McClanahan, V. P. Balema and P. S. Weiss, *ACS Nano*, 2009, **3**, 527–536.
2 G. Rojas, X. Chen, C. Bravo, J.-H. Kim, J.-S. Kim, J. Xiao, P. A. Dowben, Y. Gao, X. C. Zeng, W. Choe and A. Enders, *J. Phys. Chem. C*, 2010, **114**, 9408–9415.
3 X. S. Ke, Y. Chang, J. Z. Chen, J. Tian, J. Mack, X. Cheng, Z. Shen and J. L. Zhang, *J. Am. Chem. Soc.*, 2014, **136**, 9598–9607.
4 X. S. Ke, Y. Ning, J. Tang, J. Y. Hu, H. Y. Yin, G. X. Wang, Z. S. Yang, J. Jie, K. Liu, Z. S. Meng, Z. Zhang, H. Su, C. Shu and J. L. Zhang, *Chemistry*, 2016, **22**, 9676–9686.
5 Z.-S. Yang, Y. Ning, H.-Y. Yin and J.-L. Zhang, *Inorg. Chem. Front.*, 2018, **5**, 2291–2299.
6 Y. Ning, X. S. Ke, J. Y. Hu, Y. W. Liu, F. Ma, H. L. Sun and J. L. Zhang, *Inorg. Chem.*, 2017, **56**, 1897–1905.
7 M. Lepper, J. Köbl, T. Schmitt, M. Gurrath, A. de Siervo, M. A. Schneider, H.-P. Steinrück, B. Meyer, H. Marbach and W. Hieringer, *Chem. Commun.*, 2017, **53**, 8207–8210.
8 C.-l. Chiang, C. Xu, Z. Han and W. Ho, *Science*, 2014, **344**, 885.
9 Z. Han, G. Czap, C.-l. Chiang, C. Xu, P. J. Wagner, X. Wei, Y. Zhang, R. Wu and W. Ho, *Science*, 2017, **358**, 206.
10 E. A. Pozzi, G. Goubert, N. Chiang, N. Jiang, C. T. Chapman, M. O. McAnally, A.-I. Henry, T. Seideman, G. C. Schatz, M. C. Hersam and R. P. V. Duyne, *Chem. Rev.*, 2017, **117**, 4961–4982.
11 N. Jiang, E. T. Foley, J. M. Klingsporn, M. D. Sonntag, N. A. Valley, J. A. Dieringer, T. Seideman, G. C. Schatz, M. C. Hersam and R. P. Van Duyne, *Nano Lett.*, 2012, **12**, 5061–5067.
12 J. Lee, N. Tallarida, X. Chen, P. Liu, L. Jensen and V. A. Apkarian, *ACS Nano*, 2017, **11**, 11466–11474.
13 B. Pettinger, B. Ren, G. Picardi, R. Schuster and G. Ertl, *Phys. Rev. Lett.*, 2004, **92**, 096101.
14 R. Zhang, Y. Zhang, Z. C. Dong, S. Jiang, C. Zhang, L. G. Chen, L. Zhang, Y. Liao, J. Aizpurua, Y. Luo, J. L. Yang and J. G. Hou, *Nature*, 2013, **498**, 82.
15 J. Lee, K. T. Crampton, N. Tallarida and V. A. Apkarian, *Nature*, 2019, **568**, 78–82.
16 N. Chiang, N. Jiang, D. V. Chulhai, E. A. Pozzi, M. C. Hersam, L. Jensen, T. Seideman and R. P. Van Duyne, *Nano Lett.*, 2015, **15**, 4114–4120.
17 N. Chiang, N. Jiang, L. R. Madison, E. A. Pozzi, M. R. Wasielewski, M. A. Ratner, M. C. Hersam, T. Seideman, G. C. Schatz and R. P. Van Duyne, *J. Am. Chem. Soc.*, 2017, **139**, 18664–18669.
18 R. Zhang, X. Zhang, H. Wang, Y. Zhang, S. Jiang, C. Hu, Y. Zhang, Y. Luo and Z. Dong, *Angew. Chem., Int. Ed.*, 2017, **56**, 5561–5564.
19 S. Jiang, Y. Zhang, R. Zhang, C. Hu, M. Liao, Y. Luo, J. Yang, Z. Dong and J. G. Hou, *Nat. Nanotechnol.*, 2015, **10**, 865.
20 S. Mahapatra, Y. Ning, J. F. Schultz, L. Li, J.-L. Zhang and N. Jiang, *Nano Lett.*, 2019, **19**, 3267–3272.
21 F. Menaa, B. Menaa and O. Sharts, *Faraday Discuss.*, 2011, **149**, 269–278.
22 F. Shao, W. Dai, Y. Zhang, W. Zhang, A. D. Schlüter and R. Zenobi, *ACS Nano*, 2018, **12**, 5021–5029.
23 Y. Zhang, R. Zhang, S. Jiang, Y. Zhang and Z.-C. Dong, *ChemPhysChem*, 2019, **20**, 37–41.
24 N. Jiang, N. Chiang, L. R. Madison, E. A. Pozzi, M. R. Wasielewski, T. Seideman, M. A. Ratner, M. C. Hersam, G. C. Schatz and R. P. Van Duyne, *Nano Lett.*, 2016, **16**, 3898–3904.
25 M. Gouterman, P. M. Rentzepis and K. D. Straub, *Porphyrins, Excited States and Dynamics*, American Chemical Society, Washington, DC, 1986, DOI: 10.1021/bk-1986-0321.
26 X. Gao, J. P. Davies and M. J. Weaver, *J. Phys. Chem.*, 1990, **94**, 6858–6864.
27 W. Auwärter, D. Écija, F. Klappenberger and J. V. Barth, *Nat. Chem.*, 2015, **7**, 105.

28 J. Xiao, S. Ditze, M. Chen, F. Buchner, M. Stark, M. Drost, H.-P. Steinrück, J. M. Gottfried and H. Marbach, *J. Phys. Chem. C*, 2012, **116**, 12275–12282.
29 M. Eichberger, M. Marschall, J. Reichert, A. Weber-Bargioni, W. Auwärter, R. L. C. Wang, H. J. Kreuzer, Y. Pennec, A. Schiffrin and J. V. Barth, *Nano Lett.*, 2008, **8**, 4608–4613.
30 N. Jiang, Y. Y. Zhang, Q. Liu, Z. H. Cheng, Z. T. Deng, S. X. Du, H. J. Gao, M. J. Beck and S. T. Pantelides, *Nano Lett.*, 2010, **10**, 1184–1188.
31 S. Kawai, A. Sadeghi, F. Xu, L. Peng, A. Orita, J. Otera, S. Goedecker and E. Meyer, *ACS Nano*, 2015, **9**, 2574–2583.
32 Y. J. Feng, K. P. Bohnen and C. T. Chan, *Phys. Rev. B: Condens. Matter Mater. Phys.*, 2005, **72**, 125401.
33 X. H. Qiu, G. V. Nazin and W. Ho, *Science*, 2003, **299**, 542.
34 K. Kimura, K. Miwa, H. Imada, M. Imai-Imada, S. Kawahara, J. Takeya, M. Kawai, M. Galperin and Y. Kim, *Nature*, 2019, **570**, 210–213.
35 Z. H. Cheng, S. X. Du, N. Jiang, Y. Y. Zhang, W. Guo, W. A. Hofer and H. J. Gao, *Surf. Sci.*, 2011, **605**, 415–418.
36 W. H. Soe, C. Manzano, A. De Sarkar, N. Chandrasekhar and C. Joachim, *Phys. Rev. Lett.*, 2009, **102**, 176102.
37 P. J. Whiteman, J. F. Schultz, Z. D. Porach, H. Chen and N. Jiang, *J. Phys. Chem. C*, 2018, **122**, 5489–5495.